

Origin of colossal magnetoresistance in LaMnO₃ manganite

 HPSTAR
 147-2015

 Maria Baldini^{a,1}, Takaki Muramatsu^b, Mohammad Sherafati^c, Ho-kwang Mao^{b,d,1}, Lorenzo Malavasi^{e,f}, Paolo Postorino^g, Sashi Satpathy^h, and Viktor V. Struzhkin^b

^aHigh Pressure Synergetic Consortium, Geophysical Laboratory, Carnegie Institution of Washington, Argonne, IL 60439; ^bGeophysical Laboratory, Carnegie Institution of Washington, Washington, DC 20015; ^cInstituto de Ciencia de Materiales de Madrid, Consejo Superior de Investigaciones Científicas, Cantoblanco, E-28049 Madrid, Spain; ^dCenter for High Pressure Science and Technology Advanced Research, Shanghai 201203, China; ^eDepartment of Chemistry, University of Pavia, I-27100 Pavia, Italy; ^fItalian National Consortium for Materials Science and Technology, University of Pavia Research Unit, I-27100 Pavia, Italy; ^gDepartment of Physics, University of Rome "Sapienza," I-00185 Rome, Italy; and ^hDepartment of Physics and Astronomy, University of Missouri, Columbia, MO 65211

Contributed by Ho-kwang Mao, July 14, 2015 (sent for review November 25, 2014; reviewed by Roberto De Renzi, D. D. Sharma, and J.-S. Zhou)

Phase separation is a crucial ingredient of the physics of manganites; however, the role of mixed phases in the development of the colossal magnetoresistance (CMR) phenomenon still needs to be clarified. We report the realization of CMR in a single-valent LaMnO₃ manganite. We found that the insulator-to-metal transition at 32 GPa is well described using the percolation theory. Pressure induces phase separation, and the CMR takes place at the percolation threshold. A large memory effect is observed together with the CMR, suggesting the presence of magnetic clusters. The phase separation scenario is well reproduced, solving a model Hamiltonian. Our results demonstrate in a clean way that phase separation is at the origin of CMR in LaMnO₃.

colossal magnetoresistance | strongly correlated materials | phase separation | high pressure | transport measurements

In hole-doped rare earth manganite compounds, the colossal magnetoresistance (CMR) peaks at a transition from a high-temperature (T) insulating paramagnetic phase to a low- T conducting ferromagnetic phase. The presence of Mn³⁺ and Mn⁴⁺ ions together with the site-site double-exchange (DE) mechanism (1) appear to capture the essence of this phenomenon. A plethora of experimental and theoretical investigations have recently suggested that the ground states of manganites are intrinsically inhomogeneous and characterized by the presence of competing phases (2–8) extending over domains at nanoscale/mesoscale. High pressure (P) has a triggering effect for phase separation because either magnetic or structural domains have been observed in compressed manganites (9–12). The role of the nanostructuring and of the interdomain interactions in the CMR phenomenon is still far from being completely understood, and to design materials that incorporate CMR at room temperature (RT) remains a challenge because of the strong interplay among electronic, structural, and magnetic interactions at both atomic and interdomain scales.

As an archetypal cooperative Jahn–Teller (JT) system (13) and the parent compound of several important mixed-valence CMR manganite families, LaMnO₃ (LMO) is at the focus of intense investigations. Up to now, the CMR effect has been observed in hole-doped LMO, but not in single-valent LMO. At RT , LMO enters a high conductive phase above 32 GPa showing a “bad-metal” behavior (14). Previous Raman spectroscopy study (9) shows the emergence, in compressed LMO, of a phase-separated (PS) state consisting of domains of JT-distorted and undistorted MnO₆ octahedra. The simultaneous presence of an inherent phase separation as well as of a metallization process resembles the conditions under which CMR is observed in doped compounds, and suggests the onset of CMR in compressed LMO. To verify this hypothesis, we have carried out an extensive study of the transport properties of LMO over a wide P – T region ($12 < P < 54$ GPa and $10 < T < 300$ K) and applied magnetic field H , varying from 0 to 8 T. Here, we report the realization of CMR in a narrow pressure range between 30 and 35 GPa as the sample transforms from an

insulator to a metal. The high-pressure insulator-to-metal transition is described by a percolation mechanism within the PS state. This result demonstrates that phase separation observed at the percolation threshold is the driving force for CMR in LMO.

Results and Discussion

Electrical resistance, R , data measured in situ during the warming cycle in quasi-four-probe configuration (Fig. S1) are displayed in Fig. 1A for $H = 0$ and $H = 8$ T. Three regimes can be identified: a typical semiconductor behavior for $P < 32$ GPa; a metallic character for $P > 46$ GPa; and an intermediate- P range, $32 < P < 46$ GPa, where the metallization process and CMR are observed. This peculiar behavior can be explained by the P -tuning of the intradomain and interdomain interactions. Lattice compression induces the emergence of small ferromagnetic metallic (FM) domains (undistorted octahedra) with randomly oriented magnetization within an antiferromagnetic (AFM) insulating matrix (JT-distorted octahedra). For $P < 32$ GPa, $R(T)$ plots displays a typical insulator behavior ($dR/dT < 0$), which is consistent with a PS scenario where small FM domains are dispersed in an insulating matrix (Fig. 1B) and do not actually contribute to the system conductivity. The high- T data follow [$R = R_0 \exp(T_0/T)^{1/2}$]. This occurs due to tunneling or hopping between clusters consistently with the presence of intermixed metallic and insulating regions (15).

Significance

Magnetoresistance is the change of resistance in the presence of an external magnetic field. In rare-earth manganite compounds, this change is orders of magnitude stronger than usual and it is promising for developing new spintronic and electronic devices. The colossal magnetoresistance (CMR) effect has been observed only in chemically doped manganite compounds. We report the realization of CMR in a compressed single-valent LaMnO₃ manganite compound. Pressure generates an inhomogeneous phase constituted by two components: a nonconductive one with a unique structural distortion and a metallic one without distortion. The CMR takes place when the competition between the two phases is at a maximum. We identify phase separation as the driving force for generating CMR in LaMnO₃.

Author contributions: M.B. and V.V.S. designed research; M.B. and T.M. performed research; M.S. and S.S. performed theoretical calculation; T.M., H.-k.M., L.M., P.P., and V.V.S. contributed new reagents/analytical tools; M.B. analyzed data; M.B. and P.P. wrote the paper; and M.S. wrote the Supporting Information.

Reviewers: R.D.R., University of Parma; D.D.S., Indian Institute of Science; and J.-S.Z., University of Texas at Austin.

The authors declare no conflict of interest.

¹To whom correspondence may be addressed. Email: mbaldini@carnegiescience.edu or mao@gl.ciw.edu.

This article contains supporting information online at www.pnas.org/lookup/suppl/doi:10.1073/pnas.1424866112/-DCSupplemental.

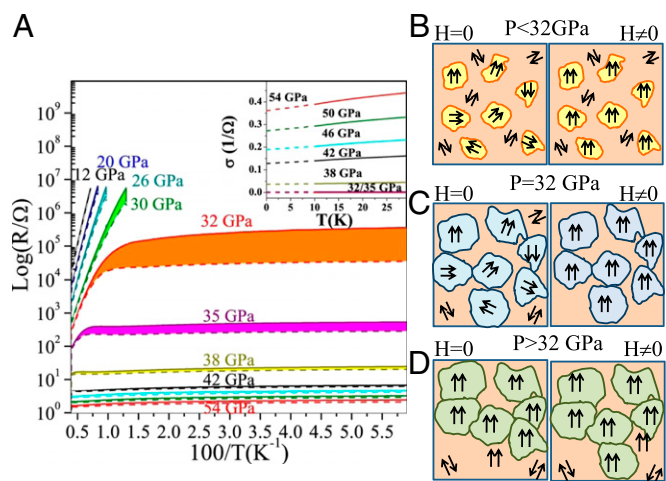


Fig. 1. (A) Temperature dependence of the resistance $\text{Log}_{10}(R/R_0)$ between 12 and 54 GPa. Solid lines are the data collected at 0 T, and dashed lines are the data collected at 8 T. (Inset) Temperature dependence of electrical conductivity: the dashed lines indicate the 0 K extrapolation. (B–D) Schematic sketches of the PS state over the three different pressure regimes. (B) $P < 32$ GPa: the volume fraction of the FM region is too small and LMO is an insulator. (C) $P = 32$ GPa: LMO is at the percolation threshold and applied magnetic field induces a spin-polarized metallic conduction and CMR. (D) $P > 32$ GPa: the extended, connected FM phase is finally established.

In the high- P regime, low- R values and positive dR/dT are observed at RT , in agreement with the formation of more homogeneous phase with large, oriented, and highly connected FM domains (Fig. 1D). Wide metallic paths are thus available for spin-polarized conduction. A residual resistance is observed at low T . The low- T data are linear in $\ln(T)$, which suggests the presence of a Kondo-like magnetic scattering mechanism (16) (Fig. S2). Kondo effect is observed also in ferromagnetic conducting compounds containing small amounts of spin-glass and/or antiferromagnetic impurities (16). However, the energy scale where the upturn takes place is really high compared with typical Kondo systems. Grain boundary effects (17, 18), magnetic frustration due to intercluster interactions, or the freezing of the spin clusters can be at the origin of the residual resistance observed at low T (15, 19, 20).

The intermediate- P region is nevertheless the most intriguing. Here, although LMO still retains a negative derivative of $R(T)$ ($dR/dT < 0$), the transition toward a high conductivity phase can be clearly identified. R is reduced by more than one order of magnitude on increasing P from 30 to 32 GPa, and by four orders of magnitude on compressing from 32 to 42 GPa (Fig. 1A). Moreover, the 0 K extrapolation of the low- T conductivity (Inset of Fig. 1A) displays values definitively greater than zero above 35 GPa, indicating the crossover from an insulating to a high conductive phase. The percolation threshold among conductive FM domains can be identified within the 32- to 35-GPa range.

The most important result is nevertheless the strong magneto-resistance $\text{MR} = [R(H=0) - R(H)]/R(H=0)$ response at around 32 GPa, where a resistance variation of more than one order of magnitude is observed for an 8-T applied magnetic field (Fig. 1A). In Fig. 2, the MR percentage vs. H is displayed. MR is around 20% at 12 GPa and continuously increases with P until it reaches the maximum value, 80%, at 32 GPa. At 35 GPa, MR drops below 40% and transport properties do not show any significant field dependence above 38 GPa, with MR being around 10%.

The appearance of CMR and its P dependence are consistent with the PS scenario discussed above. At low P , the charge

transport among weakly connected, FM clusters is further inhibited by the random orientation of their magnetization (Fig. 1B). The FM domain size is changing with the application of a magnetic field at a fixed T and P , and the effect of the magnetic field becomes more and more preeminent as the volume fraction of the FM domains grows with P (Fig. 2A–D). At 32 GPa, LMO is approaching the percolation threshold and the FM domains come into close contact. The conductivity is thus governed by very close or connected FM clusters, and the competition between metallic and insulating clusters is at a maximum (Fig. 1C). In this peculiar configuration, conduction among the metallic domains depends sensitively on the relative spin orientation of adjacent clusters, and remarkable MR originates from the field-induced alignment of FM domains (Figs. 1C and 2E). The effect of magnetic field is finally reduced with increasing P above 35 GPa, where the strong interaction among connected FM domains allows the self-alignment of their magnetization (Fig. 1D), and conductivity shows only a weak field dependence (Fig. 2F–I).

Further support to this magnetic PS scenario and to the cluster reorientation effect of the applied field is given by the hysteretic cycles detectable at 32 GPa (Fig. 2E). The memory effect is quite large. The initial R value without field is 40% higher than that one reobtained at $H = 0$ T after the application of the magnetic field due to the residual effect of field induced orientation of the domains (Fig. 2E). The competition between the AFM and FM phases has been also confirmed by ab initio calculations (21) and supported by our previous Raman results (9). The metallization process is associated with the closure of the e_g band gap and with the crossing of the Fermi level by the unoccupied t_{2g} band (21).

The PS scenario is confirmed by standard percolation theory (22, 23). Scaling laws for resistance are given by $R \propto (v - v_c)^{-t}$ and $R \propto (v_c - v)^s$ for metallic and insulating regimes respectively. Here, v is the volume fraction of the metallic phase (23). The

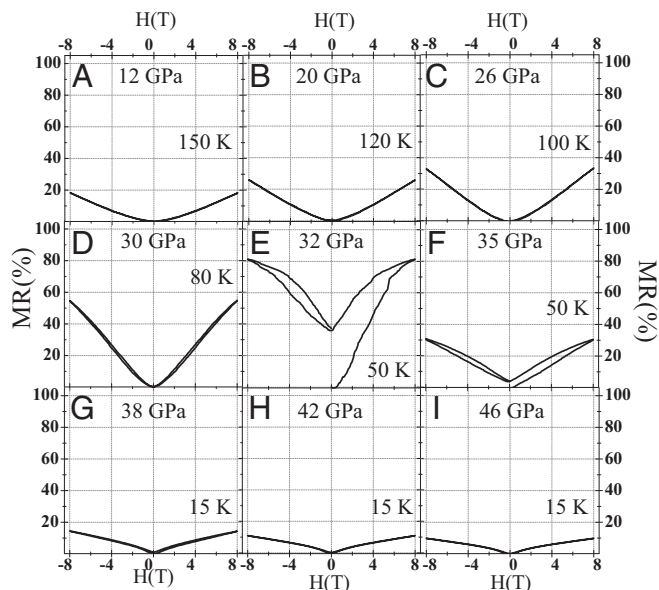


Fig. 2. MR percentage as function of pressure. (A–D) The MR percentage increases from 12 to 32 GPa. (E) At 32 GPa, the CMR effect takes place ($\text{MR} = 80\%$). (F–I) MR starts to decrease at 35 GPa, and it is less than 10% at 46 GPa. This is consistent with a continuous growth of the volume fraction of the metallic units with pressure. Magnetic field becomes more and more effective as the volume fraction of the metallic clusters increases with pressure (0–30 GPa). CMR is observed at 32 GPa just below the percolation threshold.

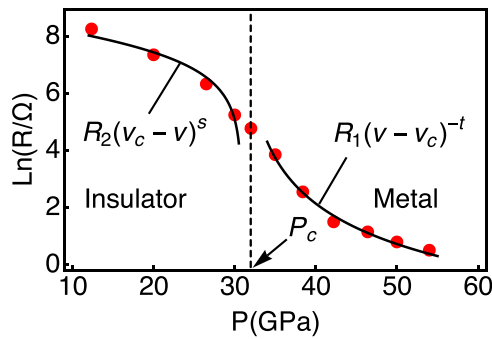


Fig. 3. Natural logarithm of resistance vs. pressure at ambient temperature. Red dots represent the experimental data. Black solid curves are the theoretical fits for $v_c = 0.29$, $t = 2.15$, and $s = 0.88$.

values of volume fractions were estimated solving a model Hamiltonian describing LMO behavior at RT (24):

$$H = \sum_{\langle ij \rangle, \alpha\beta} t_{ij}^{\alpha\beta} (\hat{c}_{i\alpha}^\dagger \hat{c}_{j\beta} + \text{H. c.}) - g \sum_i (Q_{i3} \hat{\tau}_z + Q_{i2} \hat{\tau}_x) + \frac{1}{2} K \sum_i (Q_{i3}^2 + Q_{i2}^2) + U \sum_i \hat{n}_{i1} \hat{n}_{i2}.$$

The first term represents the hopping integral and the last three terms incorporate the JT physics of the Mn e_g electrons and the coulomb interactions. The effect of pressure is accounted by a volume-dependent hopping integral ($t \propto 1/r^7$) and by adding a Madelung term ($-A/r$) and an ion-ion repulsive term (B/r^{12}) to the Hamiltonian. The Hamiltonian is solved using the Gutzwiller variational method. The calculated total energy shows a double minimum corresponding to the low- P JT distorted insulating phase and the high- P undistorted metallic phase (Fig. S3). The theoretical volume fractions of each phase were used to fit the R data collected at RT (Supporting Information and Fig. S4). Fig. 3 shows an excellent agreement between theoretical and experimental data. The predicted percolation pressure, $P_c = 31$ GPa, results close to the pressure range determined experimentally. The obtained critical exponents $t = 2.1 \pm 0.2$ and $s = 0.9 \pm 0.2$ are consistent with the expected universal values for 3D percolating systems (22).

The T - P phase diagram presented in Fig. 4 summarizes the present results. A PS phase is found over a wide P - T region. At low P , LMO remains in an insulating state. The number and the dimensions of the FM domains as well as the interaction among them grow with pressure, driving domain alignment over a large scale until an extended, connected FM phase is finally established at low T and very high P . Here, LMO displays a metallic character ($dR/dT > 0$) and weak field dependence. It is important to point out that the presence of a PS phase is essential for CMR. Indeed, the MR increases as the volume fraction of FM phase grows applying P and H and peaks at the percolation threshold where the competition between the two phases is at maximum. Here, a spin-polarized metallic conduction takes place (color map in Fig. 4). The presence of a FM phase by itself cannot explain the observed CMR. Indeed, above the percolation threshold, where the FM phase is dominant, no significant effects are observed on applying magnetic field.

This is in agreement with a unified picture pointing toward a “physics” of manganites over two different correlation lengths, namely, one at the atomic level, where the interaction is basically driven by the hopping integral, and the other at the nanoscale/mesoscale, dominated by the interactions among domains belonging to different competing phases. In many mixed-valence manganite compounds, the occurrence and the magnitude of

CMR peaks at the insulator to metal transition basically depend upon the small scale site-site interactions (25), although PS is also observed and plays a role (26, 27). The DE mechanism (1) and the interplay with the JT distortion appear to capture the essence of this phenomenon.

In the present case, the DE mechanism (1), considered the triggering microscopic interaction, is definitely inoperative. A remarkably high MR is achieved just below the percolation threshold among FM domains in pure LMO. Rather close analogies can be found in the behavior of composite artificial structures where strong negative MR is observed (15).

The relevance and the importance of both the morphology of the PS state (domain boundary surfaces, relative volumes) and the dynamics of the domains (P and T and magnetic field dependences) deserve a deeper and careful investigation. Nevertheless, our discovery has a deep impact on the physics of CMR because it demonstrates that entirely inhomogeneity-driven MR is obtained in a pure stoichiometric compound. Pressure, indeed, induces the onset of phase inhomogeneities that drive the system toward a PS state. The inherent magnetoelectric characteristics of the competing phases and the crossing of a percolation threshold are, thus, the necessary conditions for generating CMR in LMO. The remarkably strong MR measured only over a narrow region around the percolation threshold, as well as the concomitant strong memory effects sweeping the applied magnetic field, make us confident about the leading role of the PS in the magnetoconductive phenomena here observed.

We believe that the balance between small (atomic)- and large (domain)-scale interactions strongly affects the onset and the magnitude of the MR in a large variety of manganites. In particular, the role of PS and percolation transition is magnified when the competing phases show remarkably different magnetoelectric properties.

On these bases, properly shaping the interaction at the atomic level and the system inhomogeneity at the nanoscale could represent an effective route for the engineering of efficient MR materials.

Materials and Methods

LaMnO₃ sample was synthesized by solid-state reaction starting from proper amounts of La₂O₃ (Aldrich; 99.999%) and Mn₂O₃ (Aldrich; 99.999%). Pellets were prepared from the thoroughly mixed powders and allowed to react at 1,200 °C for a total time of at least 90 h, during which they were reground and repelletized at least twice. The pellet was then conditioned in argon at

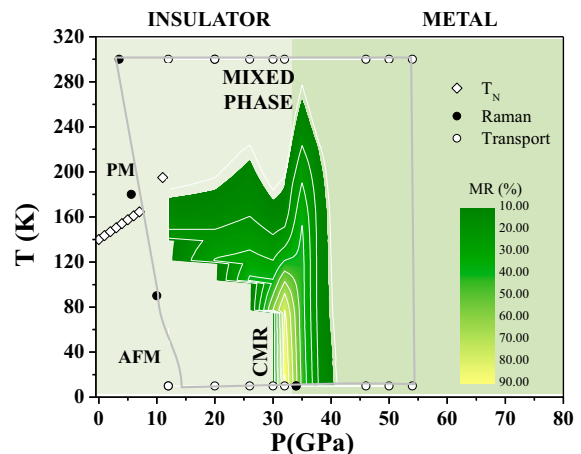


Fig. 4. Temperature vs. pressure phase diagram of LMO. White diamonds: pressure dependence of T_N (31). The black and white circles delimit the temperature and pressure regions investigated by Raman spectroscopy (9) and by transport measurements, respectively. The gray line marks the area in which domains are present. The color map delimits the P - T region in which MR is observed going from 15% variation (green) to 90% variation (yellow).

900 °C to assure the oxygen stoichiometry. Oxygen stoichiometry was determined by means of thermogravimetric analysis (28) confirming the correct LaMnO_3 stoichiometry. X-ray data were collected, and the sample has the expected Pbnm structure. Raman data collected at ambient condition also confirm the goodness of the pellet.

Magnetotransport experiments were performed using the physical properties measurement system (PPMS) facility at Geophysical Laboratory, Carnegie Institution of Washington. A miniature nonmagnetic diamond anvil cell (DAC) was used (29). A Re gasket was initially preindented using 300- μm anvils. The bottom part of the gasket chamber was then removed by laser drilling and hexagonal BN was pressed inside the chamber multiple times to cover and electrically insulate the edge of the gasket. Black Stycast epoxy was used to insulate the rest of the gasket. LMO powder was then loaded in a 70- μm hole and four platinum leads (2 μm thick) were placed in electric contact with the sample (Fig. S1). The DAC was electrically connected with PPMS resistivity puck. At each pressure, resistance data were collected

over cooling and warming temperature cycles (10–300 K) at first without and successively with an 8-T applied magnetic field.

For each pressure point, magnetoresistance $\text{MR} = R(H=0) - R(H)/R(H=0)$ data were collected at selected temperatures. MR measurements were taken sweeping the magnetic field in the following way: from $H = 0$ T to $H = 8$ T, from $H = 8$ T to $H = -8$ T, and finally from $H = -8$ T to $H = 0$ T. A standard symmetric DAC was used as an external press for applying force to PPMS-DAC. Pressure was measured using the ruby fluorescence technique (30).

ACKNOWLEDGMENTS. This work was supported as part of Energy Frontier Research in Extreme Environments Center, an Energy Frontier Research Center funded by the US Department of Energy, Office of Science under Award DE-SC0001057. S.S. acknowledges the support by the Office of Basic Energy Sciences of the US Department of Energy through Grant DE-FG02-00ER45818. M.S. is thankful for funding from the European Union Seventh Framework Programme under Grant Agreement 604391 Graphene Flagship.

- Zener C (1951) Interaction between the d -shells in the transition metals. II. Ferromagnetic compounds of manganese with perovskite structure. *Phys Rev* 82:403.
- Tao J, et al. (2011) Role of structurally and magnetically modified nanoclusters in colossal magnetoresistance. *Proc Natl Acad Sci USA* 108(52):20941–20946.
- Lai K, et al. (2010) Mesoscopic percolating resistance network in a strained manganite thin film. *Science* 329(5988):190–193.
- Fäth M, et al. (1999) Spatially inhomogeneous metal-insulator transition in doped manganites. *Science* 285(5433):1540–1542.
- Sen C, Alvarez G, Dagotto E (2007) Competing ferromagnetic and charge-ordered states in models for manganites: The origin of the colossal magnetoresistance effect. *Phys Rev Lett* 98(12):127202.
- Tao J, et al. (2009) Direct imaging of nanoscale phase separation in $\text{La}_{0.55}\text{Ca}_{0.45}\text{MnO}_3$: Relationship to colossal magnetoresistance. *Phys Rev Lett* 103(9):097202.
- Dagotto E, Hotta T, Moreo A (2001) Colossal magnetoresistant materials: The key role of phase separation. *Phys Rep* 344:1–153.
- Dagotto E (2005) Complexity in strongly correlated electronic systems. *Science* 309(5732):257–262.
- Baldini M, Struzhkin VV, Goncharov AF, Postorino P, Mao WL (2011) Persistence of Jahn-Teller distortion up to the insulator to metal transition in LaMnO_3 . *Phys Rev Lett* 106(6):066402.
- Malavasi L, et al. (2010) High pressure behavior of Ga-doped LaMnO_3 : A combined x-ray diffraction and Raman spectroscopy study. *J Mater Chem* 20:1304–1311.
- Baldini M, et al. (2012) Pressure induced tuning of magnetic phase separation in $\text{Nd}_{0.53}\text{Sr}_{0.47}\text{MnO}_3$. *Phys Rev B* 86:094407.
- Baldini M, Di Castro D, Cestelli-Guidi M, Garcia J, Postorino P (2009) Phase-separated states in high-pressure $\text{LaMn}_{1-x}\text{Ga}_x\text{O}_3$ manganites. *Phys Rev B* 80:045123.
- Goodenough J, Longo JM (1970) *Magnetic and Other Properties of Oxides and Related Compound*, Landolt-Borstein Tabellen, New Series, Group 3, eds Hellewege K-H, Hellewege AM (Springer, Berlin), Vol 4.
- Loa I, et al. (2001) Pressure-induced quenching of the Jahn-Teller distortion and insulator-to-metal transition in LaMnO_3 . *Phys Rev Lett* 87(12):125501.
- Wu J, et al. (2005) Intergranular giant magnetoresistance in a spontaneously phase separated perovskite oxide. *Phys Rev Lett* 94(3):037201.
- Zhang J, et al. (2005) Kondo-like transport and its correlation with the spin-glass phase in perovskite manganites. *Phys Rev B* 72:054410.
- Gupta A, et al. (1996) Grain-boundary effects on the magnetoresistance properties of perovskite manganite films. *Phys Rev B* 54(22):R15629–R15632.
- Xu Y, Zhang J, Cao G, Jing C, Cao S (2006) Low-temperature resistivity minimum and weak spin disorder of polycrystalline $\text{La}_{2/3}\text{Ca}_{1/3}\text{MnO}_3$ in a magnetic field. *Phys Rev B* 73(22):224410.
- Rivadulla F, López-Quintela MA, Rivas J (2004) Origin of the glassy magnetic behavior of the phase segregated state of the perovskites. *Phys Rev Lett* 93(16):167206.
- Kundu S, Nath TK (2010) Size-induced metallic state in nanoparticles of ferromagnetic insulating $\text{Nd}_{0.8}\text{Sr}_{0.2}\text{MnO}_3$. *J Phys Condens Matter* 22(50):506002.
- He J, Chen MX, Chen XQ, Franchini C (2012) Pressure effects on Jahn-Teller distortion in perovskites: The roles of local and bulk compressibilities. *Phys Rev B* 85:195135.
- Stauffer D, Aharony A (1998) *Introduction to Percolation Theory* (Taylor & Francis, London), 2nd Ed.
- Nan CW (1993) Physics of inhomogeneous inorganic materials. *Prog Mater Sci* 37:1–116.
- Sherafati M, Baldini M, Malavasi L, Satpathy S (2015) Percolative Metal-Insulator transition in LaMnO_3 . arXiv:1507.06592.
- Allodi G, et al. (2014) Band filling effect on polaron localization in $\text{La}_{1-x}(\text{Ca}_y\text{Sr}_{1-y})_x\text{MnO}_3$. *J Phys Condens Matter* 2(26):266004.
- Goodenough JB, Zhou J-S (1997) *Nature* 386:229–230.
- Sarma DD, et al. (2004) Direct observation of large electronic domains with memory effect in doped manganites. *Phys Rev Lett* 93(9):097202.
- Malavasi L, Mozzati MC, Ghigna P, Azzoni CB, Flor G (2003) Lattice disorder, electric properties, and magnetic behavior of $\text{La}_{1-x}\text{Na}_x\text{MnO}_{3+\delta}$ manganites. *J Phys Chem B* 107(11):2500–2505.
- Gavriliuk AG, Mironovich AA, Struzhkin VV (2009) Miniature diamond anvil cell for broad range of high pressure measurements. *Rev Sci Instrum* 80(4):043906.
- Mao H-K, Xu J, Bell PM (1986) Calibration of the ruby pressure gauge to 800 kbar under quasi-hydrostatic conditions. *J Geophys Res* 91:4673–4676.
- Zhou J-S, Uwatoko Y, Matsubayashi K, Goodenough JB (2008) Breakdown of magnetic order in Mott insulators with frustrated superexchange interaction. *Phys Rev B* 78:220402R.
- Bergman DJ, Stroud D (1992) Physical properties of macroscopically inhomogeneous media. *Solid State Physics: Advances in Research and Applications*, eds Ehrenreich H, Turnbull D (Academic, San Diego), Vol 46, pp 147–269.
- Marder MP (2010) *Condensed Matter Physics* (Wiley, Hoboken, NJ), 2nd Ed, section 5.3.4.
- Murnaghan FD (1944) The compressibility of media under extreme pressures. *Proc Natl Acad Sci USA* 30(9):244–247.
- Scher H, Zallen R (1970) Critical density in percolation processes. *J Chem Phys* 53:3759–3761.
- Pike GE, Seager CH (1974) Percolation and conductivity: A computer study. I. *Phys Rev B* 10:1421–1434.
- Shklovskii BI, Efros AL (1984) *Electronic Properties of Doped Semiconductors* (Springer, Berlin), section 5.3.